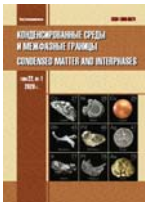

Condensed Matter and Interphases
(Kondensirovannye sredy i mezhfaznye granitsy)

DOI https://doi.org/10.17308/kcmf.2020.22/2536 eISSN 2687-0711
Received 10 February 2020
Accepted 15 March 2020
Published online 25 March 2020

Microcone Anodic Oxide Films on Sintered Niobium Powders

© 2020 N. M. Yakovleva✉[a], A. M. Shulga[a], K. V. Stepanova[a], A. N. Kokatev[a], V. S. Rudnev [b], I. V. Lukiyanchuk[b], V. G. Kuryavyi[b]

[a]*Petrozavodsk State University,*
33 Lenina prospect, Petrozavodsk 185910, Republic of Karelia, Russian Federation

[b]*Institute of Chemistry, Far-Eastern Branch of the Russian Academy of Sciences,*
159 prospect 100-letya Vladivostoka, Vladivostok 690022, Russian Federation

Abstract
Information on the anodizing of sintered powders (SP) of niobium is limited by the study of the growth of barrier-type films. The formation of a nanostructured anodic oxide film (AOF) on the surface of powder particles should lead to a noticeable increase in the specific surface of the sample and an increase in the chemical activity of the material. In view of the above, the study of the anodic nanostructuring of sintered niobium powders is of high importance and offers opportunities for creating new functional nanomaterials. This paper was aimed at the study of the anodizing process of sintered Nb powders in a fluorine-containing aqueous electrolyte 1 M H_2SO_4 + 1 % HF.
The objects of the study were samples of sintered Nb powder with a specific area of S_{spec} = 800 cm^2/g. Anodizing was conducted in a 1 M H_2SO_4 + 1 % HF electrolyte with various values of current density j_a. Surface morphology before and after anodising was investigated by scanning electron microscopy (SEM) and atomic force microscopy (AFM). X-ray diffractometry was used to study the phase composition. Kinetics of the growth of anodic oxide films (AOF) on the surface of sintered Nb powders SP in galvanostatic mode was studied. The optimal conditions were defined for obtaining $U_a(t)$ voltage-time transients, characteristic of the formation of self-organised porous anodic oxide films (AOF). It was established that anodizing at current density values j_a = 0.10–0.20 mA/cm^2 leads to the formation of a Nb_2O_5 oxide film on the surface of sintered powders SP with a regular-porous layer adjacent to metal and a crystalline microcone layer over it. The microcones (up to 0.6 μm high, up to 2 μm in effective base diameter) consist of branched fibrils with a diameter of ~18–30 nm, connected on top.
It was established for the first time that anodizing of sintered niobium powders in a fluorine-containing aqueous electrolyte leads to the formation of an oxide film with an upper crystalline microcone layer on the surface of powder microparticles. The suggested method for surface processing can be used for the development of biocompatible powder implants.

Keywords: sintered niobium powders, anodic oxide films, microcones, crystalline, nanostructured.

Funding: The study was supported by the Flagship University Development Program of the FSFEI HE Petrozavodsk State University for 2017–2021.

For citation: Yakovleva N. M., Shulga A. M., Stepanova K. V., Kokatev A. N., Rudnev V. S., Lukiyanchuk I. V., Kuryavyi V. G. Microcone anodic oxide films on sintered niobium powders. *Kondensirovannye sredy i mezhfaznye granitsy = Condensed Matter and Interphases.* 2020;22(1): 124–134. DOI: https://doi.org/10.17308/kcmf.2020.22/2536

✉ Natalia M. Yakovleva, e-mail: nmyakov@gmail.com

1. Introduction

It is known that the anodizing of Ta, Nb, Al, Ti, and other metals in weak acid water solutions that do not dissolve the oxide film being formed leads to the formation of thick (or barrier-type) anodic oxide films (AOF) with dielectric properties on their surfaces [1]. Self-organised oxide films with regularly located nanosized structural elements (tubes or pores) can also be formed on the surface of metals and alloys by electrochemical anodizing in electrolyte solutions. Self-organised AOFs are usually divided into two groups: porous and tubular with different morphological characteristics [2, 3].

Previous research showed that the synergy of the processes of the oxide film growth and dissolution implemented during the anodizing of niobium in fluorine-containing electrolytes also lead to the formation of self-organised nanoporous anodic oxide films [4–13]. The interest in nanoporous AOFs formed on Nb can be explained by such properties as high specific area, good adhesion to the substrate, biocompatibility, antibacterial, and catalytic activity. Such AOFs can be effectively used in gas sensors, catalysts, electrolytic capacitors, and electrochromic devices as well as in thin-film lithium-ion batteries, etc. [11, 13–17].

According to [15, 18–30], the anodizing of niobium foil in fluorine and phosphate containing aqueous and non-aqueous (organic) electrolytes can also help to obtain oxide films with a surface layer consisting of an ensemble of nanonstructured microcones. The oxide films with such morphology obtained by the anodising of niobium in fluorine-containing aqueous solutions were mentioned for the first time in papers [18, 19]. In a series of articles [21–23], it was shown that microcones can also be obtained by anodizing in a hot glycerine electrolyte with additives K_2HPO_4 and K_3PO_4. It was established that microcones have crystal structure corresponding to orthorhombic T-Nb_2O_5 [29] in contrast to self-organised AOFs that tend to be X-ray amorphous. Specific features of the structure of microcones have not been thoroughly studied yet, although it is shown that they consist of dendritic fibres of nanosized diameter connected on top [28–30]. Their large surface area, morphological regularity, and crystal atomic structure make them appealing for different applications. In particular, new biomedical applications, fabrication of the surfaces with regulated wettability, and the use as photoanodes in dye-sensitised solar cells are considered [28, 29]. The relative lack of information on crystalline microcone anodic niobium oxides provides motivation for the further study of their formation.

There is no agreement on the mechanism of initiation and development of microcones of crystalline Nb_2O_5 during anodizing. Only first model representations, based on the initiation and development of crystalline oxide nuclei on the metal/oxide interface, have been suggested [21, 29]. Most researchers agree that the initiation and growth of microcones of crystallites Nb_2O_5 with the formation of nanostructured microcones occur under a strong electric field in the presence of fluoride ions (with NaF and/or HF in aqueous electrolytes) or phosphate ions (with K_2HPO_4 + K_3PO_4 in organic electrolytes) with a rather long time of anodizing and/or increased temperatures of the electrolyte (T ~ 160 °C).

Previously, the growth of nanoporous and nanotubular AOFs obtained on the surface of metal foil and tin was studied. Exceptions are the works dedicated to the formation of bioactive anodic oxide coatings on the surface of porous titanium [30–32] and sintered powders of TiAl [3, 33–35]. Information available on the anodizing of sintered powders (SP) of niobium is limited by the study of the growth of barrier-type films. The formation of a nanostructured anodic oxide film (AOF) on the surface of powder particles should lead to a noticeable increase in the specific area of the sample and an increase in the chemical activity of the material. In view of the above, the study of the anodic nanostructuring of sintered niobium powders is highly important and offers opportunities for creating new functional nanomaterials.

This paper was aimed at the study of the anodizing process of sintered Nb powders in a fluorine-containing aqueous electrolyte 1 M H_2SO_4 + 1 % HF.

2. Experimental

The objects of the study were samples of sintered powder (SP) of Nb. The pressed niobium powder [36] was sintered at T = 1850 °C for 1 h. As

a result, cylindrical samples with specific area of S_{spec} = 800 cm^2/g were obtained.

The samples were preliminarily degreased in acetone and ethanol in an ultrasonic bath, washed in distilled water, and dried in the air at room temperature. Anodizing was conducted at room temperature using a three-electrode cell with a tantalum cathode and platinum counter electrode in the fluorine-containing aqueous electrolyte 1 M H_2SO_4 + 1 % HF. Anodizing was conducted in galvanostatic mode with various values of current density j_a = 0.05, 0.1, 0.15, 0.20 mA/cm^2. The process lasted 1 and 2 hours.

During the growth of the AOF, voltage-time transients $U_a(t)$ were recorded using an electronic recorder "ERBIY-7115" connected to a computer. The detailed description of the anodising technique is presented in the works [33, 37, 38].

Surface morphology of the samples before and after anodising was investigated by scanning electron microscopy (SEM) on high-resolution microscopes Mira (Tescan, Czech Republic) and S-55009 (Hitachi, Japan). Due to the fact that the anodised samples are non-conductive, their surface was preliminarily sputtered with gold.

At the same time, the elemental composition was assessed by energy dispersive X-ray analysis (EDXA) using a Thermo Scientific attachment (USA). The data was collected for 5–10 areas, including those of microscopic size (up to 50×50 μm^2) as well as the "dots" of 50×50 nm^2 and 10×10 nm^2. The areas were chosen according to the previously obtained SEM images of the surface with further quantitative analysis of the elemental composition. The thickness of the oxide films was assessed by SEM images of the samples.

At the same time, atomic force microscopy (AFM) was used to study the structure of the surface of the samples. The studies were conducted in air on a Solver Next (ZAO NT-MDT, Russia) scanning probe microscope (SPM) in tapping mode. High-resolution diamond-like carbon tips (NSG01) with the length of 125 μm, resonance frequency of 87–230 kHz, and curvature radius of the needle of 10 nm were used. The size of the scan area varied in the range from 1 to 25 μm^2 taking into account the inhomogeneous surface relief of the powder samples. Generally, fairly homogeneous areas were selected for surface scanning. From 2 to 5 areas of the surface were scanned. Using the image processing module, Image Analysis P9, of the SPM Solver Next, a primary image processing was conducted (first, filtration using a Gaussian 3×3 0.391 linear filter and a Hybrid Median non-linear filter, then image skew was corrected using the Fit Lines method of Flatten Correction 1-D for colour correction), and size distribution of the image objects (using Grain Analysis) was assessed [39].

X-ray diffractometry was used to study the phase composition. The samples were studied using the X-ray technique before and after anodising on a D8 ADVANCE (Bruker, Germany) automated diffractometer using Cu$K\alpha$ radiation in the angular range 2θ = (10–90)° with 0.02° step. To identify the phase composition of the AOF, a set of d-spacings, calculated according to the experimental data, was compared to the corresponding values for Nb and crystalline modifications of niobium oxides. For that purpose, a search programme EVA with a PDF-2 (Powder Diffraction File; Kabekkodu, 2007) database was used.

3. Results and discussion

Anodizing of sintered Nb powders in a fluorine-containing aqueous electrolyte was conducted for the first time. Initial conditions for the formation of anodic oxide films (AOF) were chosen using the data, obtained during the study of anodizing of niobium foil. According to [4], in order to obtain nanoporous AOFs in the water solution 1 M (10 wt%) H_2SO_4 with addition of (0.5–2) wt% HF, it is preferable to use the voltstatic mode at the voltage U_a = 20 V, room temperature of the electrolyte $T = T_r$ = (20–25) °C, and the process duration t_a from 30 min to 1 h. The use of such conditions of niobium foil anodising allowed obtaining a self-organised porous AOF with the diameter of open pores d_p ~ 10–30 nm and the thickness δ not exceeding 450–500 nm [12].

Taking into account this information, an electrolyte, 1 M H_2SO_4 +1 % HF, was selected for the anodizing of sintered powders (SP). By varying the current density and anodizing time of the galvanostatic process, it was established that at the current density values in the range of j_a = 0.05–0.20 mA/cm^2 and t_a = 1–2 hours the type

of voltage-time transients $U_a(t)$ is typical for the formation of self-organised porous AOFs (Fig. 1). There are successively distinguished sections of $U_a(t)$ curves that correspond to different stages of the formation of oxide films: growth of a barrier layer, initiation and self-organisation of pores, and the steady-state growth of the porous layer [2].

As j_a increases, both the growth rate of voltage at the stage of formation of the barrier layer and the time of transition to steady-state growth increase. For instance, if the time of transition to the stage of steady-state growth is approximately 2 hours with j_a= 0.05 mA/cm^2 (Fig. 1, curve *1*), then with bigger values of j_a it takes from 40 minutes to 1 hour. In all the cases, the value of steady-stage voltage is similar to the value U_a^{stat} ~ 70 V. However, U_a^{stat} tends to decrease slightly with the growth of j_a. It should be noted that the presence of numerous voltage peaks at the stage of the steady-state growth of pores is characteristic of $U_a(t)$ obtained at j_a = 0.20 mA/cm^2 (Fig. 1, curve 4). Such voltage behaviour can be caused by a local breakdown in the barrier layer [21].

During the next stage, a microscopic study of the surface morphology of the samples of sintered Nb powders before and after anodizing at j_a = 0.10 mA/cm^2 (t_a = 1 hour) was conducted using SEM. Fig. 2a shows that the microparticles have irregular shapes with linear dimensions from 10 to 40 μm. The study of the elemental composition using EDXA showed the presence of O in the quantity from 1.8 to 7.0 wt% alongside Nb on all the studied areas.

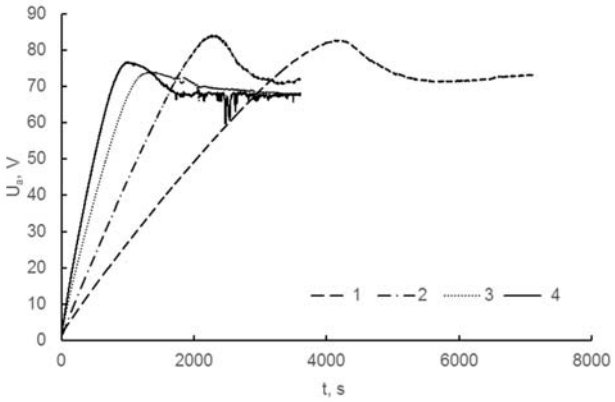

Fig. 1. $U_a(t)$ transients obtained during anodising of sintered Nb powders in the 1 M H_2SO_4 + 1% HF electrolyte with different values of current density j_a: curve 1 – j_a = 0.05 mA/cm^2 (t_a = 2 h) and curves 2, 3, 4 – j_a = 0.1, 0.15, 0.2 mA/cm^2 (t_a = 1 h)

SEM overview images of sintered Nb powders show that the surface morphology changes after anodizing: a multitude of continuously located microinhomogeneities appear (Fig. 2b). A more detailed study (Fig. 3) revealed that the discovered objects are closely located cone-shaped formations with sizes ranging from 0.4 to 2 μm, the so-called microcones (Fig. 3a). In their turn, microcones consist of branched (dendritic) fibres of nanosized diameter ~18–30 nm (fig. 3b,c) connected on top.

Fig. 3a shows that the AOF on the surface of the particles has a heterogeneous structure. From

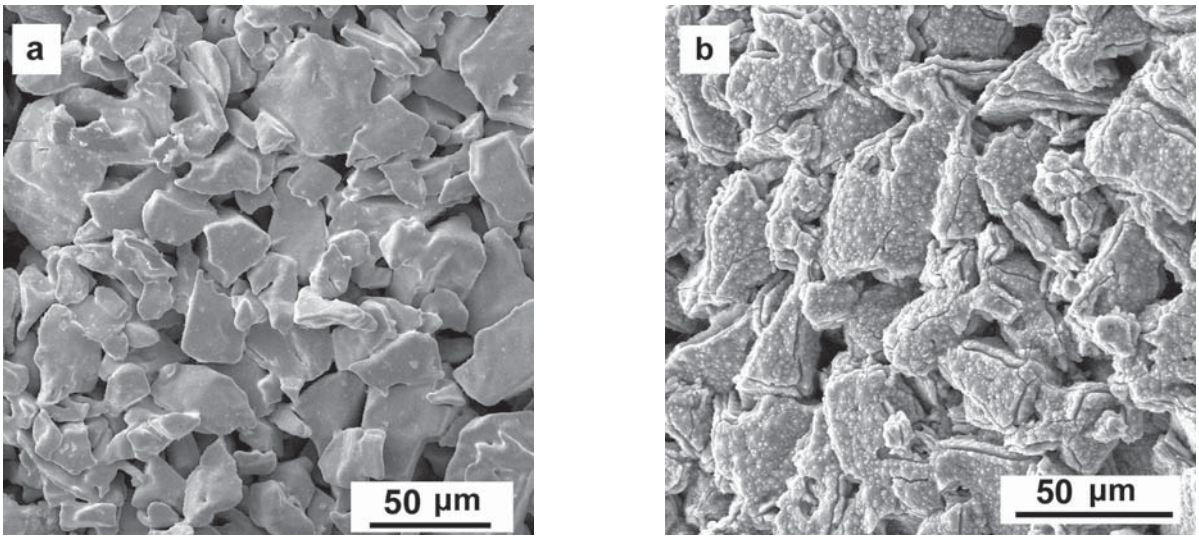

Fig. 2. SEM images of the surface of sintered Nb powder samples before (a) and after anodizing in the 1 M H_2SO_4 + 1 % HF solution for 1 hour with j_a = 0.1 mA/cm^2 (b)

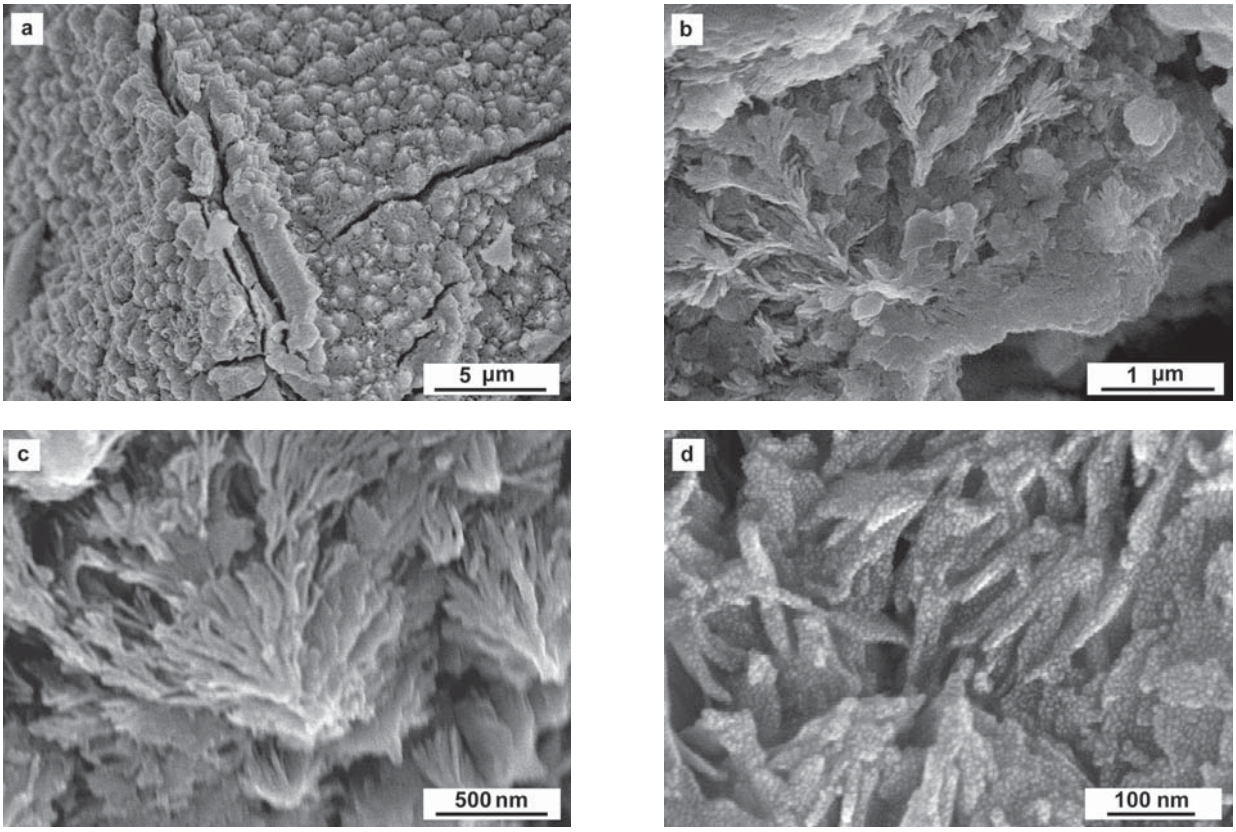

Fig. 3. SEM images of the surface of the anodizing samples of sintered Nb powders obtained at various magnifications. Anodising conditions: j_a = 0.1 mA/cm^2, t_a = 1 h, T = T_r

the side adjacent to the substrate, there is a self-organised porous oxide film of approximately 1 μm consisting of barrier and porous layers. On top of it, there is an inhomogeneous microcone layer. The height of the microcones varies from ~0.1 to 0.6 μm. As Fig. 3d shows, there are round fragments of ~ 2–8 nm in the body of nanofibers that the microcones consist of. Therefore, it can be assumed that the nanofiber has a "fine texture".

Computer processing of the SEM images of the surface area $S \approx 50$ μm^2 (Fig. 4a) allowed assessing the distribution of microcones by size, more specifically by effective base diameter d_o (Fig. 4b). It is evident that there are microcones on the selected surface area with d_o ranging from 0.45 to 1.85 μm. As the type of distribution demonstrates, ~ 40 % of the microcones have d_o in the range of 0.7–0.9 μm and ~ 30 % in the range of 1.0 to 1.3 μm. There are also ~ 30 % of the objects with 0.4 μm < d_o < 0.7 μm. The weighted mean value of the effective base diameter equals $\langle d_o \rangle$ = 0.85 μm. Thus, a significant variation of the value d_o is typical for the microcone layer of AOF.

The elemental composition of the AOF was identified by EDXA (depth of analysis up to 1 μm) for the regions of different sizes. Fig. 5 shows the results for the analysed area $S \approx 15$ μm^2. According to the obtained data, Nb and O form a part of the AOF (Fig. 5b). Also, an insignificant amount of F was found in some areas. The presence of F can be caused by the inclusion of fluorine-containing complexes into the porous oxide layer of AOF during its growth [15]. The values of weight percent of the elements $C_{Nb} \approx 70$ wt%, $C_0 \approx 30$ wt%, (Fig. 5b) show that the composition of the AOF corresponds quite well with Nb_2O_5. The obtained result was close to the EDXA data received during the study of the composition of the microcone layers formed by the anodizing of Nb foil in fluorine-containing aqueous electrolytes [19, 25, 30].

Then, the phase compositions of the samples, before and after anodizing, were studied using the X-ray method. X-ray patterns of all the studied samples after anodizing show a number of low-intensity additional lines in addition to the reflections from the niobium substrate. The identification of diffraction lines on the X-ray

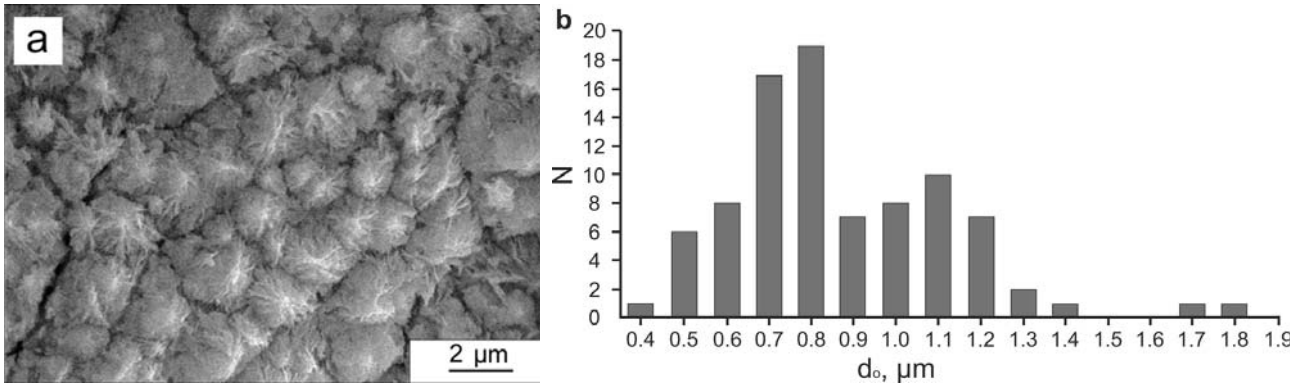

Fig. 4. a) SEM image of the surface area of the anodizing sample of the sintered Nb powder; b) the corresponding distribution of oxide microcones by sizes over effective base diameters of d_o. Anodizing conditions: j_a = 0.1 mA/cm^2, t_a = 1 h, $T = T_r$

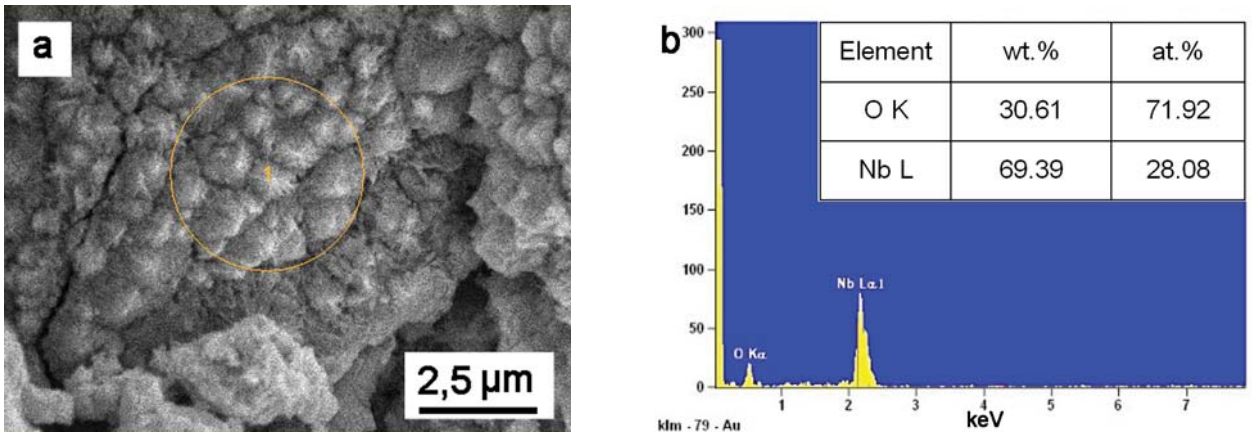

Fig. 5. a) SEM image of the surface area after anodizing; b) EDAX spectrum and composition of the analysed area

patterns of the anodized sintered powders is quite a complicated task, firstly, due to the low intensity of diffraction lines and, secondly, due to the coincident positions of several Bragg reflections for different crystalline phases of niobium oxides. Nevertheless, the comparison of the obtained values of d-spacings with the tabular data allows for the conclusion that the phase composition corresponds to the orthorhombic modification T- Nb_2O_5, which correlates to the results of the comprehensive study of the atomic structure of microcone AOFs on niobium foil in the work [28].

In our previous works [38, 39] it was shown that the AOF formed on the surface of sintered Nb powder possesses super-hydrophilic properties, high corrosion resistance in the solution modelling blood plasma, as well as improved protein adsorption. Therefore, the products made from sintered niobium powder and anodised by the developed technology can be used as biocompatible implants.

At the same time, atomic force microscopy (AFM) was used to study the structure of the surface of the samples before and after anodizing at different values of j_a. The appearance of AFM images of sintered Nb powder demonstrates that the surface has quite a developed relief and is characterised by the presence of elongated ("fibrous") formations. The width of the "fibres" is in the range from 80 to 160 nm and the length is in the range from 200 to 300 nm. A similar structure of sintered Nb powders is also revealed on SEM images of sintered Nb powders [37]. It appears that such surface morphology can be explained by special aspects of the production of cylindrical samples from sintered niobium powder.

After anodizing for 1 hour at j_a = 0.05 mA cm^2, of the surface relief practically does not change, which is likely to be related to the fact that the barrier layer of the AOF is formed during this period of time (Fig. 1, curve 1). When t_a is increased to 2 hours (Fig. 6b), a change in the

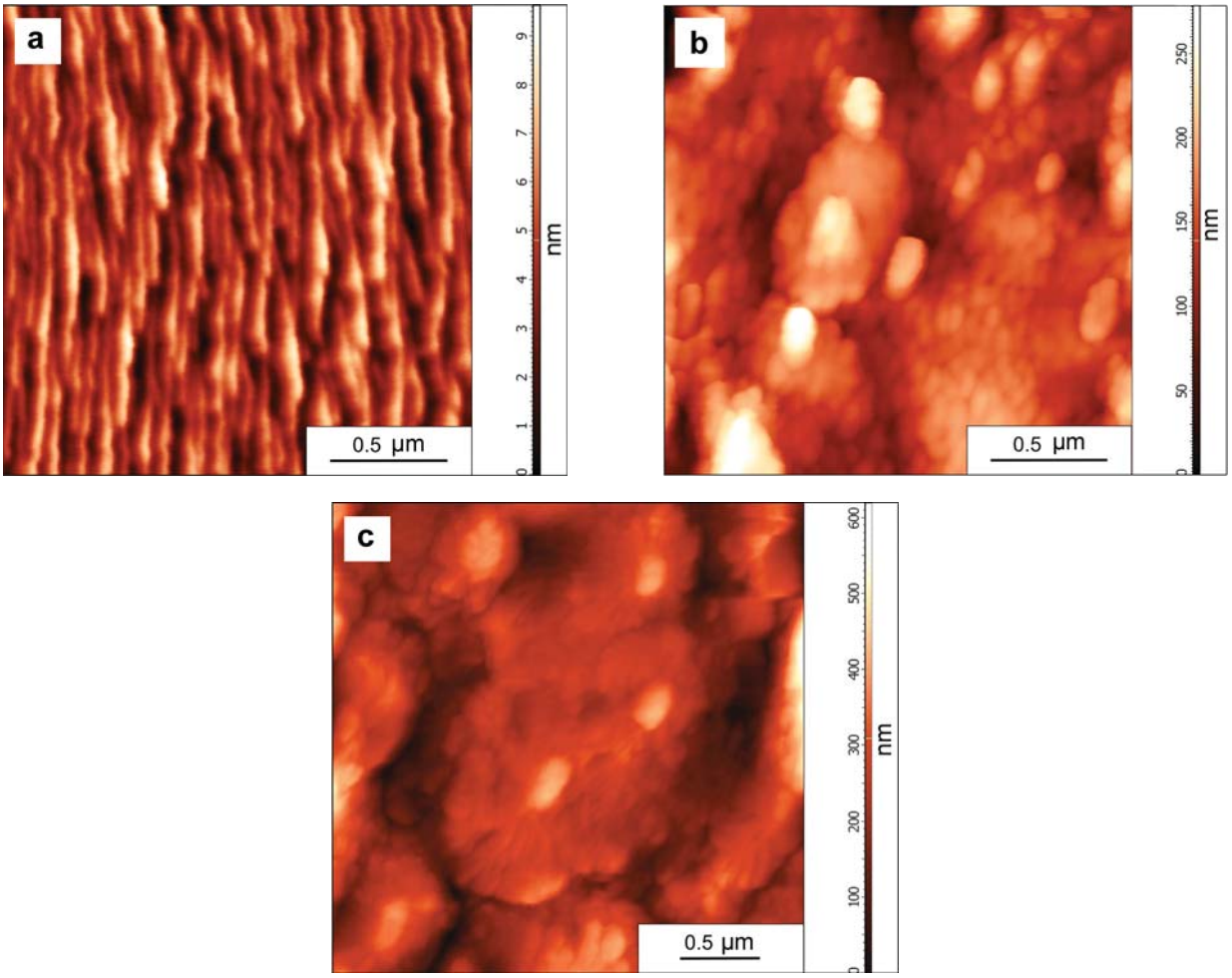

Fig. 6. AFM images of sintered Nb powders before (a) and after anodizing in 1 MH_2SO_4 +1% HF with different values of current density: b) 0.05 mA/cm^2, t_a = 2 h; c) 0.1 mA/cm^2 (t_a = 1 h)

relief is observed. In addition to the surface areas characterised by the presence of regular open pores (d_p ~ 10–20 nm), there are also unevenly located microcones of different sizes. Effective base diameters of d_o range from 150 to 600 nm. The height of the microcones varies from 50 to 300 nm. It follows that after 2 hours of anodising at j_a = 0.05 mA/cm^2, a porous oxide film is formed on the powder microparticles with individual microcone formations on its surface.

As Fig. 6c shows, the morphology of the AOF formed at j_a = 0.1 mA/cm^2 for t_a = 1 h is similar to that revealed by SEM (Fig. 3a). Closely located microcone formations of different sizes are observed on the surface of the AOF. The assessment of sizes of the bases of the microcones provides values ranging from 0.3 to 1.3 μm and heights of 0.3–0.6 μm, which correlates well with the data obtained when processing the corresponding SEM images (Fig. 3, 4).

AFM images of surface areas of the AOFs formed for 1 hour at high values of current density 0.15 mA/cm^2 and 0.2 mA/cm^2 are presented in Fig. 7a, b. Ensembles of round microcone formations with the height of 0.6 μm are observed on the surface of the AOF. It should be highlighted that while the result of anodizing at j_a = 0.05 mA/cm^2 (t_a = 2 h) on top of the regular porous layer of the AOF is only the presence of individual microcones, at j_a = 0.10–0.20 mA/cm^2 (t_a = 1 h) they completely cover the surface of the film.

The analysis of the distribution of the microcones by effective base diameters of d_b for surface areas with S = 25 μm^2 (Fig. 7c) shows that for the AOFs formed at j_a = 0.15 mA/cm^2 (Fig. 7a), ~ 80 % of the microcones have values of d_o in the range from 0.2 to 0.4 μm, while the weighted mean value of the effective base diameter equals $\langle d_o \rangle \approx 0.34$ μm. For the AOFs obtained at j_a = 0.2 mA/cm^2, the value of d_o for ~ 50 % of the microcones

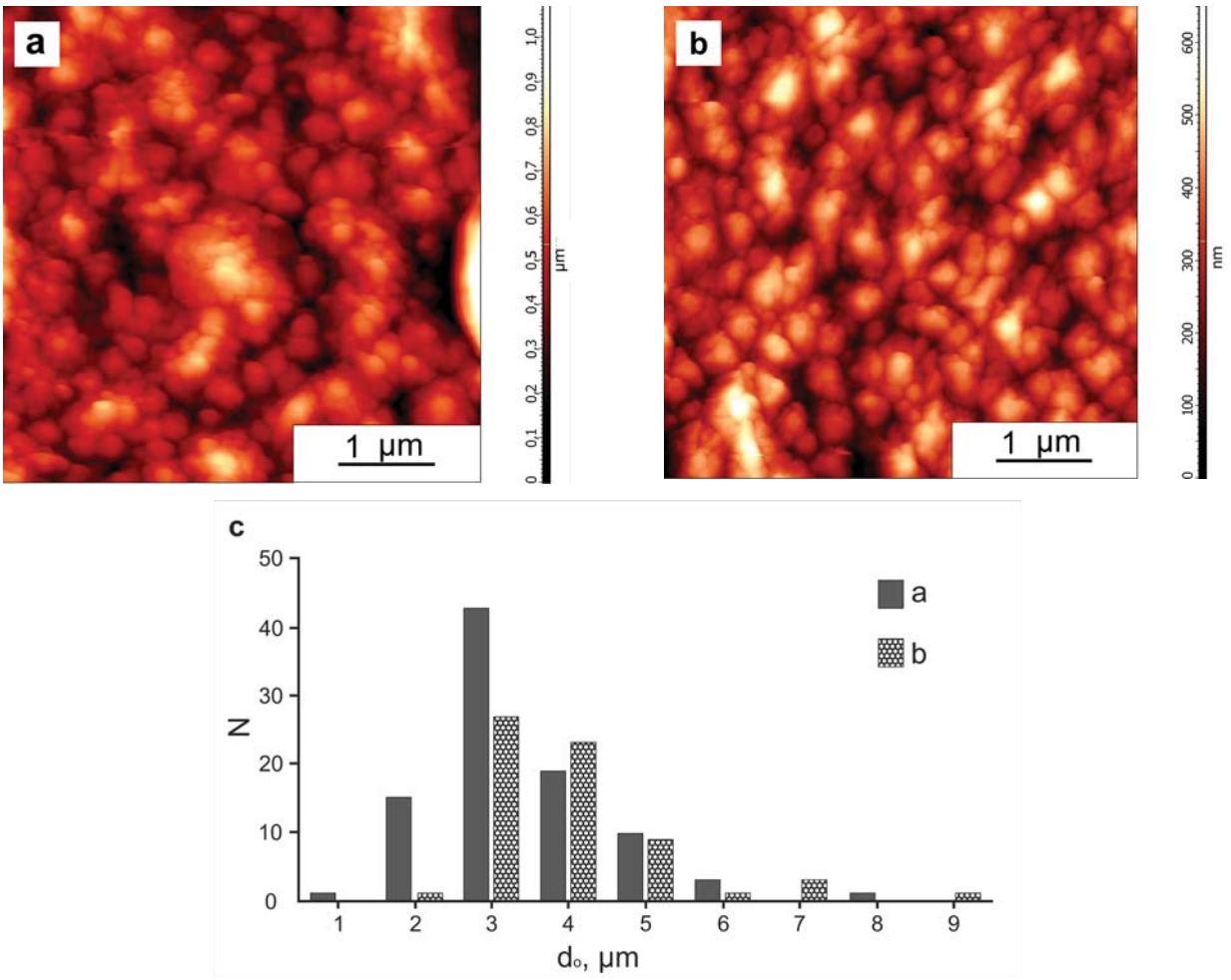

Fig. 7. AFM images of the surface of sintered Nb powders after anodizing in 1 M H_2SO_4 +1% HF (t_a = 1 h) with different values of current density: a) 0.2 mA/cm^2; b) 0.15 mA/cm^2; c) corresponding distributions of oxide microcones by size

is in the range from 0.2 to 0.3 μm, while ~ 20 % of them have 0.3 μm < d_o < 0.4 μm. In this case, the weighted mean value is $\langle d_o \rangle$ ≈ 0.29 μm. As for the AOFs formed for 1 hour at j_a = 0.15 and 0.20 мА/см^2, the microcone layer is characterised by a more homogeneous distribution of microcones by sizes as compared to the same distribution for the AOF formed at j_a = 0.1 mA/cm^2 (Fig. 4).

Such microstructures were previously found in the surface layer of the AOF during the anodizing of niobium foil in different electrolytes [7, 15, 18–20, 26, 29, 30], including aqueous solutions of H_2SO_4 with the addition of HF [18, 20, 26]. Generally, in order to obtain a continuous microcone layer, the anodizing of these electrolytes was conducted in voltstatic mode with the voltage from 20 to 60 V and at room temperature, but with a higher concentration of HF (1.5–2 wt%) or an increased duration of the process t_a = 5–12 h. For example, in [26], when anodizing niobium foil in the electrolyte 1 M H_2SO_4+ 1 wt% HF with the voltage U_a = 60 V, a microcone layer with d_o ~ 3–5 μm was formed during t_a = 5 h. Also, the size of the microcones formed on the foil in the electrolytes of similar composition is much bigger as compared to the microcone layers on sintered Nb powders.

Therefore, the anodizing of sintered Nb powders at j_a = 0.1–0.2 mA/cm^2 in a fluorine-containing aqueous electrolyte (1 M H_2SO_4 + 1 % HF) at room temperature for 1 hour forms a continuous crystalline microcone layer on the surface of the AOF. In order to obtain AOF with similar morphology on the surface of niobium foil, it usually requires either considerable time of anodizing or increasing the temperature of the electrolyte [20, 21, 26]. Existing ideas [21, 29] about the initiation and development of microcones in the process of anodizing of

niobium foil consider field crystallisation on the metal/AOF barrier layer interface as the main reason for their development. In the process of anodising of sintered Nb powders, the number of nuclei of the crystalline oxide phase of Nb_2O_5, formed under a strong electric field at the metal/oxide interface alongside with the growth of the barrier layer of AOF, will be much higher than in the process of anodizing foil. Apparently, this is caused by the developed relief of powder grains (high specific area of the sintered powder) as well as by substantial presence of oxide in their surface layer [40, 41], which is confirmed by EDXA results.

Therefore, in the process of anodizing sintered Nb powders in a fluorine-containing aqueous electrolyte in galvanostatic mode, with a current density in the range of j_a = 0.1–0.2 mA cm^2, a multilayer oxide film is formed on the surface of powder microparticles in the form of a complex of barrier and regular nanoporous layers adjacent to the substrate and upper crystalline microcone layer. Therefore, it can be said that using the developed technique of galvanostatic anodizing of sintered Nb powders, a new type of oxide crystalline microstructures can be obtained.

4. Conclusions

The anodizing of sintered niobium powder in the fluorine-containing aqueous electrolyte 1 M H_2SO_4 + 1 % HF in galvanostatic mode was studied for the first time. Through the study of the kinetics of growth of an AOF, it was established that the anodizing process (j_a = 0.05–0.20 mA/cm^2, t_a = 1–2 h, T = 21–25 °C) is characterised by transients of $U_a(t)$ typical for the formation of porous and tubular anodic oxide films. Using SEM and AFM methods, it was established that anodizing of sintered niobium samples under such conditions leads to the formation of a heterogeneous AOF with a total thickness of about 2 μm on top of a regular porous oxide layer of which there is a layer consisting of crystalline nanostructured microcones. The super-hydrophilicity, corrosion resistance in biomedia, as well as high level of protein adsorption confirm the potential of the suggested anodic modification technique for the creation of biocompatible powder implants.

Acknowledgements

The authors are grateful to Semenova L. A. and Yakovlev A. N. for their valuable consultations and participation in discussions.

Conflict of interests

The authors declare that they have no known competing financial interests or personal relationships that could have influenced the work reported in this paper.

References

1. Odynets L. L., Orlov V. M. *Anodnye oksidnye plenki* [Anodic oxide films]. Leningrad: Nauka; 1990. 200 p. (in Russ.)

2. Yakovleva N. M., Kokatev A. N., Chupakhina E. A., Stepanova K. V., Yakovlev A. N., Vasil'ev S. G., Shul'ga A. M. Surface nanostructuring of metals and alloys. Part 1. Nanostructured anodic oxide films on Al and Al alloys. *Kondensirovannye sredy i mezhfaznye granitsy = Condensed Matter and Interphases*. 2015;17(2): 137–152. Available at: https://journals.vsu.ru/kcmf/article/view/56 (In Russ., abstract in Eng.)

3. Yakovleva N. M., Kokatev A. N., Stepanova K. V., Yakovlev A. N., Chupakhina E. A., Shul'ga A. M., Vasil'ev S. G. Surface nanostructuring of metals and alloys. Part 2. Nanostructured anodic oxide films on Ti and Ti alloys. *Kondensirovannye sredy i mezhfaznye granitsy = Condensed Matter and Interphases*. 2016;18(1): 6–27. Available at: https://journals.vsu.ru/kcmf/article/view/104 (In Russ., abstract in Eng.)

4. Sieber I., Hildebrand H., Friedrich A., Schmuki P. Formation of self-organized niobium porous oxide on niobium. *Electrochemistry Communications*. 2005;7: 97–100. DOI: https://doi.org/10.1016/j.elecom.2004.11.012

5. Choi J., Lim J. H., Lee S. C., Chang J. H., Kim K. J., Cho M. A. Porous niobium oxide films prepared by anodization in HF/H_3PO_4. *Electrochimica Acta*. 2006;51: 5502–5507. DOI: https://doi.org/10.1016/j.electacta.2006.02.024

6. Tzvetkov B., Bojinov M., Girginov A., Pébère N. An electrochemical and surface analytical study of the formation of nanoporous oxides on niobium. *Electrochimica Acta*. 2007;52: 7724–7731. DOI: https://doi.org/10.1016/j.electacta.2006.12.034

7. Tzvetkov B., Bojinov M., Girginov A. Nanoporous oxide formation by anodic oxidation of Nb in sulphate–fluoride electrolytes. *J Solid State Electrochem*. 2009;13: 1215–1226. DOI: https://doi.org/10.1007/s10008-008-0651-y

8. Yoo J. E., Choi J. Surfactant-assisted growth of anodic nanoporous niobium oxide with a grained surface. *Electrochimica Acta*. 2010;55: 5142–5147. DOI: https://doi.org/10.1016/j.electacta.2010.04.021

9. Wei W., Lee K., Shaw S., Schmuki P. Anodic formation of high aspect ratio, self-ordered Nb_2O_5 nanotubes. *ChemComm*. 2012;48: 4244–4246. DOI: https://doi.org/10.1039/C2CC31007D

10. Kim H.-K., Yoo J. E., Park J., Seo E. W., Choi J. Formation of Niobium Oxide Film with Duplex Layers by Galvanostatic Anodization. *Bull. Korean Chem. Soc.* 2012;33(8): 2675–2678. http://dx.doi.org/10.5012/bkcs.2012.33.8.2675

11. Yoo J. E., Park J., Cha G., Choi J. Micro-length anodic porous niobium oxide for lithium-ion thin film battery applications. *Thin Solid Films*. 2013;531: 583–587.

12. Shul'ga A. M., Yakovleva N. M., Kokatev A. N., Stepanova K. V., Khanina E. Ya. Anodic surface nanostructuring of tantalum and niobium. *Trudy Kol'skogo nauchnogo tsentra RAN. Khimiya i materialovedenie* [Transactions of the Kola Science Centre of the Russian Academy of Science. Chemistry and material science]. 2015;5(31): 498 – 500. (In Russ.)

13. Minagar S., Berndt C. C., Wen C. Fabrication and characterization of nanoporous niobia, and nanotubular tantala, titania and zirconia via anodization. *J. Funct. Biomater.,* 2015;6: 153–170. DOI: https://doi.org/10.3390/jfb6020153

14. Ryshchenko I. M., Lyashok I. V., Gomozov V. P., Vodolazhchenko S. A., Deribo S. G. Formation of nanostructures on the basis of porous anodic niobium oxide. *Functional materials.* 2019;26(4): 729–733. DOI: https://doi.org/10.15407/fm26.04.729

15. Alias N., Rosli S. A., Hussain Z., Kian T. W., Matsuda A., Lockman Z. Anodised porous Nb_2O_5 for photoreduction of Cr(VI). *Materials Today: Proceedings.* 2019;17: 1033–1039. DOI: https://doi.org/10.1016/j.matpr.2019.06.505

16. Yao D. D., Rani R. A., O'Mullane A. P., Kalantar-Zadeh K., Ou J. Z. High performance electrochromic devices based on anodized nanoporous Nb2O5. *J. Phys. Chem. C.* 2014;118(1): 476-481. DOI: https://doi.org/10.1021/jp410097y

17. Rani R. A., Zoolfakar A. S., O'Mullane A. P., Austina M. W., Kalantar-Zadeh K. Thin films and nanostructures of niobium pentoxide: fundamental properties, synthesis methods and applications. *J. Mater. Chem. A.* 2014;2: 15683–15703. DOI:10.1039/c4ta02561j

18. Karlinsey R. L. Preparation of self-organized niobium oxide microstructures via potentiostatic anodization. *Electrochemistry Communications.* 2005;7: 1190–1194. DOI: https://doi.org/10.1016/j.elecom.2005.08.027

19. Karlinsey R. L. Self-assembled Nb2O5 microcones with tailored crystallinity. *J. Mater. Sci.* 2006;41: 5017–5020. DOI: https://doi.org/10.1007/s10853-006-0135-3

20. Zhao J., Wang X., Xu R., Mi Y., Li Y. Preparation and growth mechanism of niobium oxide microcones by the anodization method. *Electrochem. Solid-State Lett.* 2007;10(4): 31–33. DOI: DOI: https://doi.org/10.1149/1.2458528

21. Oikawa Y., Minami T., Mayama H., Tsujii K., Fushimi K., Aoki Y., Skeldon P., Thompson G. E., Habazaki H. Preparation of self-organized porous anodic niobium oxide microcones and their surface wettability. *Acta Materialia.* 2009;57: 3941–3946. DOI: https://doi.org/10.1016/j.actamat.2009.04.050

22. Yang, S., Aoki Y., Habazaki H. Effect of electrolyte temperature on the formation of self-organized anodic niobium oxide microcones in hot phosphate–glycerol electrolyte. *Applied Surface Science.* 2011;57: 8190–8195. DOI https://doi.org/10.1016/j.apsusc.2011.01.041

23. Yang S., Habazaki H., Fujii T., Aoki Y., Skeldon P., Thompson G. E. Control of morphology and surface wettability of anodic niobium oxide microcones formed in hot phosphate–glycerol electrolytes. *Electrochimica Acta.* 2011;56: 7446–7453. DOI: https://doi.org/10.1016/j.electacta.2011.07.005

24. Jung E., Chang J. H., Jeong B.-Y. Fabrication of niobium oxide nanorods by the anodization method. *Journal of the Korean Electrochemical Society.* 2011;14(4): 196–200. DOI: https://doi.org/10.5229/JKES.2011.14.4.196

25. Jeong B.-Y., Jung E. H. Micro-mountain and nano-forest pancake structure of Nb_2O_5 with surface nanowires for dye-sensitized solar cells. *Met. Mater. Int.* 2013;19(3): 617–622. DOI: https://doi.org/10.1007/s12540-013-3035-5

26. Skatkov, L., Lyashok L., Gomozov V., Tokareva I., Bayrachniy B. Anodic formation of nanoporous crystalline niobium oxide. *J. Electrochem. Sci. Eng.* 2014;4(2): 75–83. DOI: https://doi.org/10.5599/jese.2014.0050

27. Jeong B.-Y., Junga E.-H., Kim J.-H. Fabrication of superhydrophobic niobium pentoxide thin films by anodization. *Applied Surface Science.* 2014;307: 28–32. DOI: https://doi.org/10.1016/j.apsusc.2014.03.111

28. Shaheen B. S., Davenport T. C., Salem H. G., Haile S. M., Allam N. K. Rapid and controlled electrochemical synthesis of crystalline niobium oxide microcones. *MRS Communications.* 2015;5(03): 495–501. DOI https://doi.org/10.1557/mrc.2015.43

29. Bianchin A. C. V., Maldaner G. R., Fuhr L. T., Beltrami L. V. R., Malfatti C. F., Rieder E. S., Kunst S. R., Oliveira C. T. A model for the formation of niobium structures by anodization. *Materials Research.* 2017;20(4): 1010–1023. DOI: http://dx.doi.org/10.1590/1980-5373-MR-2016-0392

30. Wally Z. J., van Grunsven W., Claeyssens F., Goodall R., Reilly G. C. Porous titanium for dental implant applications. *Metals.* 2015;5: 1902–1920; DOI: https://doi.org/10.3390/met504190

31. Kulkarni M., Mazare A., Gongadze E., Perutkova Š., Kralj-Iglic V., Milošev I., Schmuki P., Iglic A.,

Mozetic M. Titanium nanostructures for biomedical applications. *Nanotechnology*. 2015;26: 1–18. DOI https://doi.org/10.1088/0957-4484/26/6/062002

32. Kokatev A. N., Stepanova K. V., Yakovleva N. M., Tolstik V. E., Shelukhina A. I., Shulga A. M. Self-organisation of a bioactive nanostructured oxide layer on the surface of sintered titanium sponge powder subjected to electrochemical anodisation. *Technical Physics*. 2018;88(9): 1377–1383. DOI: https://doi.org/10.21883/JTF.2018.09.46424.25-18

33. Stepanova K. V., Yakovleva N. M., Kokatev A. N., Pettersson H. Nanoporistye anodno-oksidnye plenki na poroshkovom splave Ti-Al [Nanoporous anodic oxide films on Ti-Al powder alloy]. *Uch.zap. PetrGU.* Seriya Estestvennye i tekhnicheskie nauki. 2015;147(2): 81–86. Available at: http://uchzap.petrsu.ru/files/n147.pdf (In Russ., abstract in Eng.)

34. Stepanova K. V., Yakovleva N. M., Kokatev A. N., Pettersson H. Influence of annealing on the structure of nanoporous oxide films on the surface of titanium–aluminum powder alloy. *Journal of Surface Investigation. X-ray, Synchrotron and Neutron Techniques*. 2016;10(5): 933–941. DOI: https://doi.org/10.7868/s0207352816090134 (In Russ.)

35. Stepanova K. V., Yakovleva N. M., Kokatev A. N., Pettersson H. The structure and properties of nanoporous anodic oxide films on titanium aluminide. *Kondensirovannye sredy i mezhfaznye granitsy = Condensed Matter and Interphases*. 2019;21(1): 135–145. DOI: https://doi.org/10.17308/kcmf.2019.21/724

36. GOST 26252-84. *Poroshok niobievyy. Tekhnicheskie usloviya*. Moscow: Izdatel'stvo standartov; 1990. 47 p. (In Russ.)

37. Shul'ga A. M., Yakovleva N. M., Kokatev A. N., Pettersson H. Nanostrukturirovannye anodno-oksidnye plenki na spechennykh poroshkakh niobiya [Nanostructured anodic oxide films on sintered niobium powders]. In: *Sbornik nauchnykh statey "Nanostruktury v kondensirovannykh sredakh"*. Minsk: Institut teplo- i massoobmena imeni A. V. Lykova NAN Belarusi; 2016. pp. 366–370. (In Russ.)

38. Yakovleva N. M., Stepanova K. V., Kokatev A. N., Shul'ga A. M. Chupakhina E. A., Vasil'ev S. G. Electrochemical anodising of sintered powders of metals and alloys. *Trudy Kol'skogo nauchnogo tsentra RAN. Khimiya i materialovedenie* [Transactions of the Kola science centre of the Russian Academy of Science] Iss. 2. P. 1. *The third all-Russian conference with international participation dedicated to the 60th anniversary of the Tananaev Institute of Chemistry and Technology of Rare Elements and Mineral Raw Materials of the Russian Academy of Sciences Kola Science Centre "Research and development in chemistry and technology of functional materials"*. Apatity: FPFIS FRC "KSC of RAS" Publ.; 2018;1(9): 479 – 484. (in Russ.)

39. Modul' obrabotki izobrazheniy Image Analysis P9: spravochnoe rukovodstvo. Moscow: NT-MDT; 2014. 482 p. (In Russ.)

40. Habazaki H., OgasawaraT., Konno H., Shimizu K., Nagata S., Skeldon P., Thompson G. E. Field crystallization of anodic niobia. *Corrosion Science*. 2007;49(2): 580–593. DOI: https://doi.org/10.1016/j.corsci.2006.06.005

41. Habazaki H., Yamasaki M., Ogasawara T., Fushimi K., Konno H., Shimizu K., Izumi T., Matsuoka R., Skeldon P., Thompson G. E. Thermal degradation of anodic niobia on niobium and oxygen-containing niobium. *Thin Solid Films*. 2008;516(6): 991–998. DOI: https://doi.org/10.1016/j.tsf.2007.06.127

Information about the authors

Natalia M. Yakovleva, DSc in in Physics and Mathematics, Full Professor, Petrozavodsk State University, Petrozavodsk, Republic of Karelia, Russian Federation; e-mail: nmyakov@petrsu.ru, nmyakov@gmail.com. ORCID iD https://orcid.org/0000-0003-4294-0183

Alisa M. Shul'ga, Engineer, Petrozavodsk State University, Petrozavodsk, Republic of Karelia, Russian Federation; e-mail: shulga.alisa@gmail.com. ORCID iD https://orcid.org/0000-0002-3844-7110

Kristina V. Stepanova, PhD in Technology, Engineer, Petrozavodsk State University, Petrozavodsk, Republic of Karelia, Russian Federation; e-mail: lady.cristin4ik@yandex.ru. ORCID iD https://orcid.org/0000-0002-4737-497X lady.cristin4ik@yandex.ru. ORCID iD https://orcid.org/0000-0002-4737-497X

Alexander N. Kokatev, PhD in Technology, Engineer, Petrozavodsk State University, Petrozavodsk, Republic of Karelia, Russian Federation; e-mail: nelanoksid@bk.ru. ORCID iD https://orcid.org/0000-0002-9449-1482

Vladimir S. Rudnev, DSc in Chemistry, Institute of Chemistry, Far-Eastern Branch of the Russian Academy of Sciences, Vladivostok, Russian Federation; e-mail: rudnevvs@ich.dvo.ru. ORCID iD https://orcid.org/0000-0002-1953-5617

Irina V. Lukiyanchuk, PhD in Chemistry, Senior Researcher, Institute of Chemistry, Far-Eastern Branch of the Russian Academy of Sciences, Vladivostok, Russian Federation; e-mail: lukiyanchuk@ich.dvo.ru. ORCID iD https://orcid.org/0000-0003-1680-4882

Valeriy G. Kuryavyi, PhD in Chemistry, Senior Researcher, Institute of Chemistry, Far-Eastern Branch of the Russian Academy of Sciences, Vladivostok, Russian Federation; e-mail: kvg@dvo.ru. ORCID iD: https://orcid.org/0000-0002-7129-8129

All authors have read and approved the final manuscript.

Translated by Marina Strepetova.
Edited and proofread by Simon Cox.